Chapter 12

METHODS for INVESTIGATING BASIC PROCESSES and CONDITIONS AFFECTING WIND EROSION

E. L. Skidmore, L. J. Hagen, D. V. Armbrust, A. A. Durar, D. W. Fryrear, K. N. Potter, L. E. Wagner, T. M. Zobeck

INTRODUCTION

Although past wind erosion research has been reasonably accepted and implemented, we need to improve our technology for measuring erosion and monitoring soil transport; replace empirical annual soil-loss models with process-based event models; better understand the soil aggregation process as influenced by inherent soil properties, soil management, cropping sequence, climate, and the changes in aggregate status seasonally and during an erosion event; determine probabilities and establish confidence limits for predicting duration and intensity of meteorologic conditions conducive to erosion; and develop user friendly prediction systems that operate on personal computers for conservation planning and resource inventory.

Because it is not feasible to incorporate the new research and technology into existing models or variations thereof, the U.S. Department of Agriculture (USDA) has charged a group of scientists to develop a new "Wind Erosion Prediction System," WEPS (*53, 55*). In this chapter, various members of that USDA core team review some of the methods used for investigating basic processes and conditions affecting wind erosion.

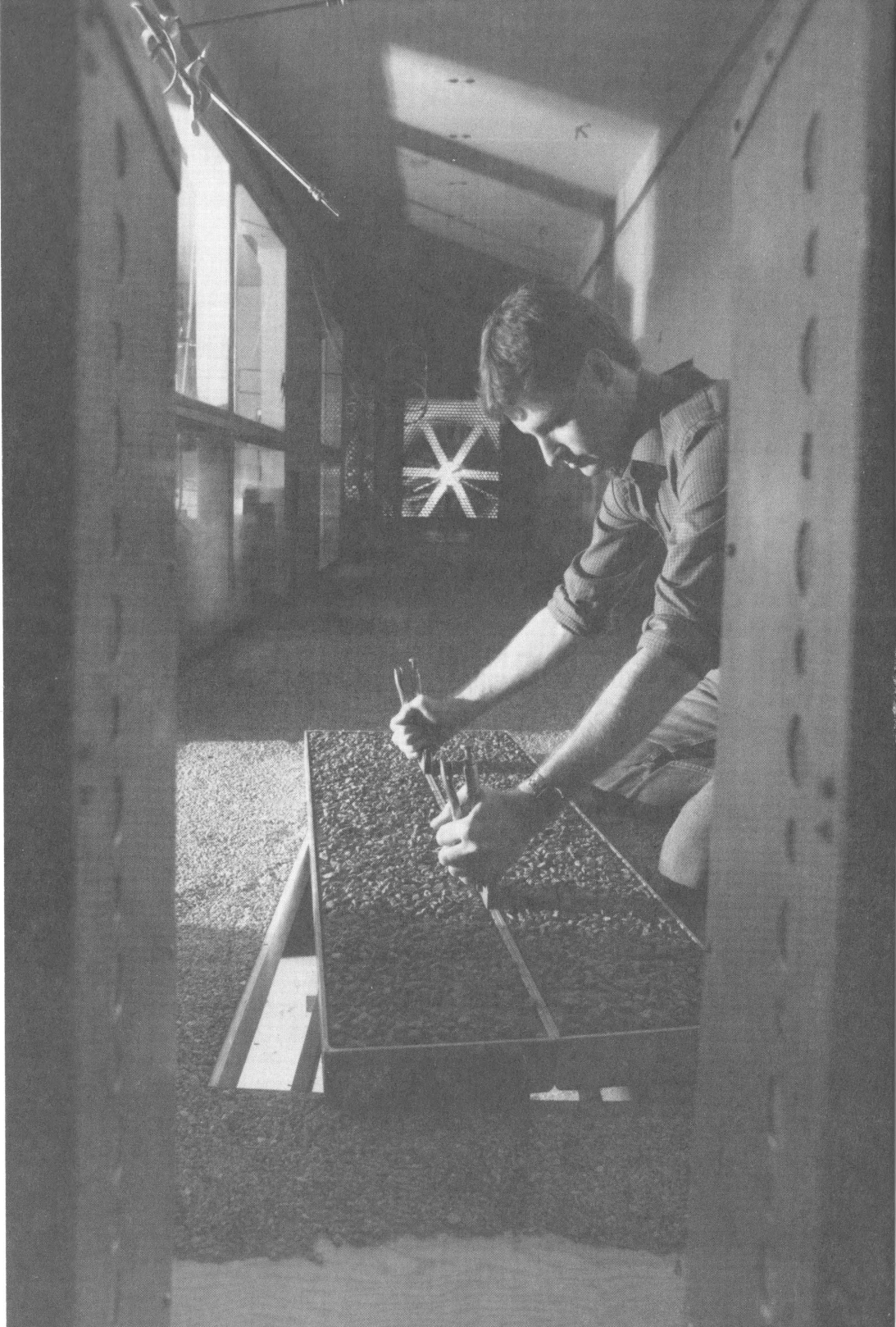

WIND DATA BASES AND SIMULATION

The need to know about the wind has prompted several studies, particularly by those interested in wind as a source of energy (*35, 57, 89*) and those concerned with erosion of soil by wind (*75, 76, 98, 100, 104, 105, 125*).

Skidmore (*98*) computed wind erosion force vectors from frequency of occurrence of direction by wind speed groups. The wind erosion force vectors were used to compute monthly magnitudes of wind erosion forces, prevailing wind erosion direction, and preponderance of wind erosion forces in the prevailing wind erosion direction. These factors indicate, respectively, potential need for wind erosion protection, proper orientation of erosion control measures, and relative merits of proper orientation of the control methods. They were furnished by month for locations throughout the United States (*106*). The resulting handbook has since been used for conservation planning and wind erosion prediction. The prevailing wind erosion direction and preponderance data are included in the recent SCS *National Agronomy Manual* (*106*). In that manual, magnitude of wind erosion forces was presented in an erosive wind energy distribution format as developed by Bondy et al. (*9*) and Lyles (*75*).

Although such wind analyses were essential for conservation planning and wind erosion prediction with the wind erosion model of Woodruff and Siddoway (*124*), they are not adequate for the evolving wind erosion technology (*53, 54, 55*). Skidmore and Tatarko (*103*) developed a wind data base suitable for use in the stochastic approaches in the current wind erosion modeling effort. Their procedure was to use monthly wind speed and wind direction summaries to calculate wind speed distribution parameters for each of 16 directions. In addition, ratios of maximum to minimum hourly wind speed, and hour of maximum wind speed, wind direction, and hourly wind speed were stored in the data base.

A stochastic wind speed/direction simulator was developed which uses data from the data base (*104*). Stochastic wind direction is determined by comparing a random number with the cumulative wind direction distribution. Once wind direction is simulated, Equation 1 is solved to determine daily mean wind speed, UMEAN

$$\text{UMEAN} = c\left\{-\ln[1 - F(u) - F_0)/(1 - F_a)]\right\}^{1/k} \qquad [1]$$

where c and k are monthly Weibull scale and shape wind speed distribution parameters (*118*); F(u) is cumulative Weibull distribution function and has a value between 0 and 1.0 assigned to it from random number generation, and F_0 is the frequency of calm periods. Wind speed at any hour of the day [U(I)] can be simulated from

$$U(I) = UMEAN + 0.5(UMAX - UMIN)\cos[2\pi(24 - HRMAX) + I)/24] \quad [2]$$

where UMAX and UMIN are daily maximum and minimum wind speeds, and HRMAX is the hour of the day when wind speed is maximum.

An output of a few simulations is illustrated in Table 12.1. Wind speed was printed every two hours for each simulation. If wind speed at any time exceeded 8 m/s, then it was flagged by a "yes" in the last column of Table 12.1. This means that wind speed is high enough to cause erosion from an unprotected surface of highly erodible particles, and an erosion submodel should be activated.

PARTICLE DETACHMENT AND TRANSPORT

Detachment and transport of particles during wind erosion are controlled by a number of static and dynamic forces interacting with a wide range of particle sizes in a turbulent flow. This discussion will present a brief overview of the various processes that occur during wind erosion and then review some of the laboratory methods used to investigate them.

Processes

The various processes that compose wind erosion are difficult to study at a point in space and time, so measurements usually represent either quasi-steady state or time integrations of detachment and transport processes over some finite space. One can visualize wind erosion for a finite space near the surface on a typical agricultural soil (control volume) as the conservation of mass of two species (saltation and creep) with two sources (emission of loose particles and abrasion of particles from clods and crust) and two sinks (trapping of saltation/creep and suspension of fine particles) (Figure 12.1). As wind erosion proceeds, rearrangement of the soil surface also occurs. Simplified surfaces are often used in laboratory studies so that individual processes can be investigated. This can be accomplished by manipulating surface roughness and selecting both composition and size of erodible and nonerodible fractions.

The forces acting on a loose grain on a particle bed at the threshold of motion are illustrated in Figure 12.2. For particles below 10 um, forces of adhesion dominate in keeping a particle on the bed, whereas for particles above 100 um, weight dominates (*85*). Single spheres much larger than sand grains have been instrumented with transducers and placed on a bed of similar spheres to study drag and lift forces (*19, 30*).

Table 12.1. Wind direction and wind speed simulation for March & July, Lubbock, Texas (*104*).

WIND	HOUR OF DAY												
DIRECTION	1	3	5	7	9	11	13	15	17	19	21	23	EROSION
MARCH	Windspeed (m/s)												
13	3.3	3.2	3.3	3.7	4.1	4.6	5.0	5.1	5.0	4.6	4.1	3.7	NO
11	4.6	4.4	4.6	5.1	5.7	6.4	6.9	7.0	6.9	6.4	5.7	5.1	NO
13	2.7	2.6	2.7	3.0	3.4	3.8	4.1	4.2	4.1	3.8	3.4	3.0	NO
4	6.2	5.9	6.2	6.8	7.7	8.6	9.3	9.5	9.3	8.6	7.7	6.8	YES
9	6.9	6.7	6.9	7.7	8.7	9.7	10.4	10.7	10.4	9.7	8.7	7.7	YES
11	8.0	7.7	8.0	8.9	10.0	11.2	12.0	12.4	12.0	11.2	10.0	8.9	YES
10	5.4	5.2	5.4	6.0	6.8	7.6	8.1	8.3	8.1	7.6	6.8	6.0	YES
12	1.7	1.7	1.7	1.9	2.2	2.4	2.6	2.7	2.6	2.4	2.2	1.9	NO
5	3.4	3.3	3.4	3.7	4.2	4.7	5.1	5.2	5.1	4.7	4.2	3.8	NO
7	7.3	7.0	7.3	8.1	9.2	10.2	11.0	11.3	11.0	10.2	9.2	8.1	YES
JULY													
5	2.4	2.1	2.0	2.0	2.1	2.4	2.7	2.9	3.1	3.1	2.9	2.7	NO
9	7.2	6.4	6.0	6.0	6.4	7.2	8.1	8.9	9.4	9.4	8.9	8.1	YES
9	4.6	4.1	3.8	3.8	4.1	4.6	5.2	5.7	6.0	6.0	5.7	5.2	NO
9	8.0	7.2	6.7	6.7	7.2	8.0	9.1	10.0	10.5	10.5	10.0	9.1	YES
6	5.7	5.1	4.7	4.7	5.1	5.7	6.4	7.0	7.4	7.4	7.0	6.4	NO
10	8.2	7.3	6.8	6.8	7.3	8.2	9.2	10.2	10.7	10.7	10.2	9.2	YES
7	3.6	3.2	2.9	2.9	3.2	3.6	4.0	4.4	4.6	4.6	4.4	4.0	NO
9	5.0	4.5	4.1	4.1	4.5	5.0	5.7	6.2	6.5	6.5	6.2	5.7	NO
12	3.0	2.6	2.5	2.5	2.6	3.0	3.3	3.7	3.9	3.9	3.7	3.3	NO
9	5.6	4.9	4.6	4.6	4.9	5.6	6.3	6.9	7.2	7.2	6.9	6.3	NO

Directions are clockwise starting with 1 - north, 2 - north, north east, etc.

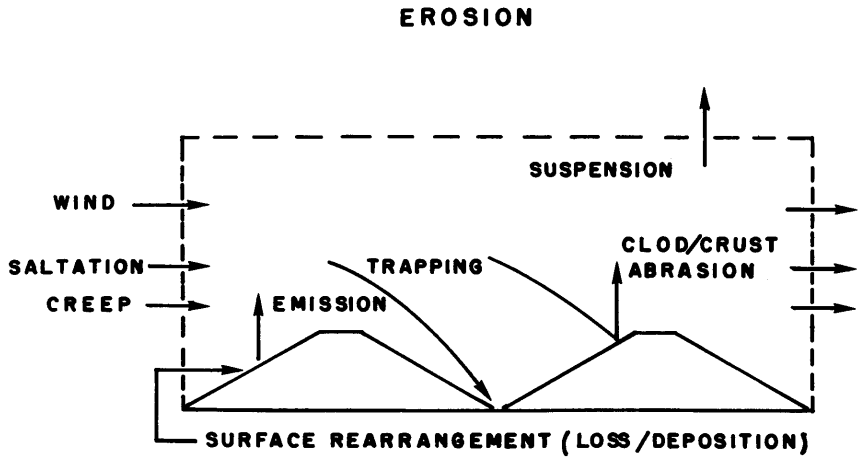

Figure 12.1 Diagram of wind erosion processes on a bare soil.

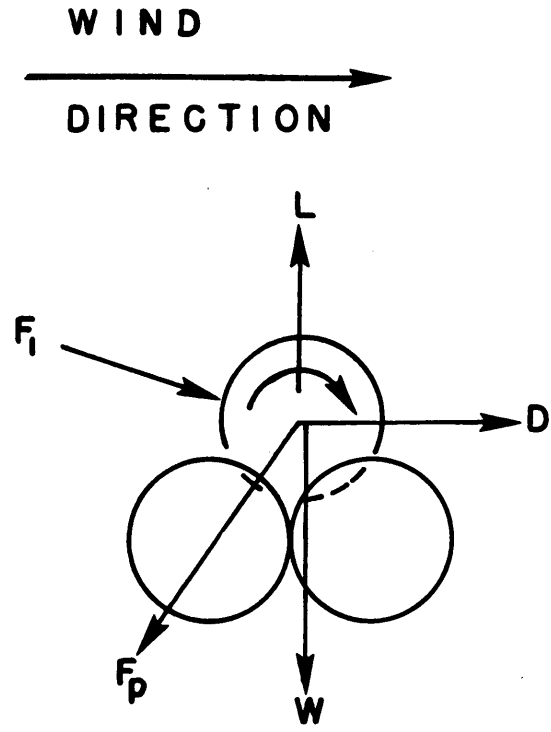

Figure 12.2 Diagram of forces acting on a single particle at the threshold of motion including aerodynamic lift (l), drag (D), moment (M), weight (W), interparticle cohesive force (F_p), and force of impact from an incoming particle (F_I).

Wind tunnels

Environmental wind tunnels are often used to study detachment and transport. These are generally characterized by a long test section designed to develop a turbulent boundary layer whose velocity profile and turbulence characteristics match those of the modeled atmospheric boundary layer. These also often include an adjustable top that can be sloped to remove the pressure gradient down the working section. Even with long test sections, however, it is sometimes necessary to augment boundary layer depth with upstream turbulence generators (*108*). Attempts to adapt short, aerodynamic tunnels to atmospheric simulation have met with mixed success (*84*).

Maintaining similitude while modeling the effects of blowing particles is a problem because of the large number of variables. The variables are generally arranged in dimensionless groups and, in a true model, all the groups have the same value in the model as in the full scale (*66, 68*). Frequently, it is impossible to maintain a true model, such as with snow drifting near windbreaks, and a distorted model must be used. In this case, the degree of distortion must be varied in the experiments and extra care is needed to extrapolate the results to full scale. Recent results show that the Froude number is one of the most important dimensionless parameters when simulating particle transport (*64*).

Threshold

Monitoring initial motion of the particles also has been accomplished by visual observation. However, improved precision is gained by using instrumentation, such as the laser optical system described by Nickling (*83*). He also described an analytical interpretation of the threshold velocity from the sensor output. A transducer with a vertical array of piezoelectric crystals attached to an electronic counter is another instrument that has been used to sense both threshold velocities and momentum of particles (*48*). Finally, low saltation rates have been measured with saltation sand catchers and a saltation threshold discharge defined as 0.001 kg $m^{-1}s^{-1}$ (*78*).

On complex surfaces composed of erodible particles and nonerodible elements, the shearing stress is distributed between the erodible and nonerodible elements (*74*). Even for complex surfaces, however, a surface threshold velocity can be measured. Surface threshold velocities for simulated stubble (*76*), aggregate cover (*73*), and tillage ridges (*56*) have been investigated. Another technique in threshold studies is to use a narrow range of erodible particles and let the wind uncover buried nonerodible elements.

When removal ceases, one can infer that the friction velocity in the sheltered zones is equal to the erodible particle threshold velocity.

Saltation

The saltation process can be investigated by a number of methods. Trajectories of individual saltating particles have been theoretically predicted by numerical integration of the equations of motion. When Magnus lifting force due to particle spin was included, theory agreed well with observations (*120, 121*). Experimental measurements of particle trajectories were obtained from analysis of high-speed motion pictures at 2000 to 10,000 frames/s. In the latter study, particle speeds passing a constant height also were measured using a velocimeter, which consisted of a light source and two phototransistors. The instrument was based on a design modified from Schmidt (*95*). Numerical models of saltating particle trajectories also have been combined with measurements of vertical profiles of the saltation flux to predict such parameters as particle launch velocities and surface dislodgement rates (*107*).

The progress of saltating particles moving downwind can be observed for groups of particles by using dyed grains (*122*) or for an individual particle by using a radioactive tracer (*8*). Methods to prepare, observe, and separate variable size and density sands for saltation studies have been presented by Gerety and Slingerland (*44*). Transport capacity of saltating particles by wind has been measured both outdoors and in wind tunnels using sand catchers. Various empirical formulas have been developed relating the transport capacity to friction velocity (*49*).

Erosion

A convenient way to study abrasion is to place trays of soil in a wind tunnel and blow abrader from an upwind source across them. The abrasion flux from unit surface area (G_{ab}) for a surface composed of n classes of target materials has been modeled as

$$G_{ab} = \left(\sum_{i=1}^{n} F_i \, C_{ai} \right) q \qquad [3]$$

where C_{ai} is an abrasion coefficient with units (L^{-1}), F_i is the fraction of saltation impacting the ith material, and q is saltation discharge ($ML^{-1}T^{-1}$) (*54*). Abrasion coefficient depended mainly on the abrasion resistance of target clods or crust and was only slightly dependent on wind speed or type of abrader. By placing various fractions of non-abradable clods on a crusted surface, values for F_i were calculated after measuring the other three parameters in Equation 3.

AGGREGATE STABILITY

Dry soil-aggregate stability and aggregate-size distribution are primary factors affecting soil susceptibility to wind erosion. Aggregate density, to a lesser extent, affects soil erodibility but is much less variable than stability and size distribution. Soil-aggregate stability and size distribution vary widely in time and space. From Table 12.7 (*124*), it is seen that nonaggregated sandy soils with only one percent of the sand having diameters greater than 0.84 mm are 10 and 100 times more erodible than aggregated soils with 53 and 77 percent of their aggregates greater than 0.84 mm, respectively. Similarly, dry aggregate stability may differ a hundredfold between soils. This section and the next one discuss measuring both of these transient soil properties.

Various methods based on different principles have been used to evaluate dry aggregate stability. Principles include relative aggregate size reduction from applied forces, rupture stress, and energy consumed in size reduction. In the relative size reduction technique, the aggregates were subjected to external forces in several ways: (a) placing in metal cylinders that were inverted end-over-end 20 times (*14*); (b) repeated rotary sieving (*16*); and (c) vigorous sieving with flat sieves (*112*). For rupture stress measurement, aggregates were diametrically loaded between parallel plates (*91, 92, 102*).

Energy consumed in size reduction has been measured using several different methods. The desire to know the work required to subdivide aggregates into smaller units, led Marshall and Quirk (*79*) to use a drop-shatter method. Air-dried samples were shattered by dropping them onto a concrete floor from various heights. The kinetic energy was dissipated by impact with the hard surface. Others (*36, 46, 50*) have used the drop-shatter technique to establish the relationship between the energy imparted to the soil and the degree of fragmentation.

Skidmore and Powers (*102*) measured the energy consumed in crushing an aggregate by integrating the area under the force against a distance curve. Boyd et al. (*10*) developed a soil-aggregate crushing-energy meter, for measuring the energy consumed in crushing an aggregate.

Skidmore et al. (*103, 104*) evaluated four different measures of aggregate stability. The names and unit of measurement for each of these methods were: crushing-energy/surface-area (J/m^2), crushing energy (J/kg), rupture stress (kPa), and initial break force (N). Crushing-energy/surface-area represents the work done in crushing an aggregate divided by the new surface area exposed, which gave energy per unit of surface area. The surface area was calculated by using the arithmetic mean of each of the sieve size fractions and assuming that the aggregates were spherical. The crush-

ing energy was calculated by dividing the work done in crushing an aggregate by the mass of the aggregate being crushed. The rupture stress was calculated by dividing the initial break force by the cross-sectional area of the aggregate. This required an independent measurement of aggregate density. The initial break force was simply the force on the aggregate at initial fracture.

Coefficient of variation for crushing energy (J/kg) < crushing energy/surface area (J/m2) < rupture stress (kPa) < initial break force (N). These four methods correlated reasonably well. When regressed on each other, the coefficients of determination ranged from 0.90 to 0.97. Sample numbers required to estimate the true mean within 25 percent of the mean at 0.05 level of significance were 10, 12, 20, and 22 for crushing energy, crushing-energy/surface area, rupture stress, and initial break force, respectively.

In general, the ranking of simplicity-of-measurement is in the same order as sample numbers required to estimate the mean value. The initial break force is easiest to measure but requires the greatest number of measurements. For the crushing-energy/surface-area method, work required to break aggregate bonds and the newly created external surface area are measured. This method also had the greatest range, more than two orders of magnitude, between the soft and hard soils. One of the drawbacks of this method is the tedium of measuring the new surface area exposed as a result of the crushing.

The energy consumed in size reduction of the crushing-energy method was also measured, but instead of dividing by new surface exposed, the crushing energy was divided by the mass of the aggregate, thus making it more important to crush to the same end point each time. In spite of that, this method required the fewest aggregates for an estimate of the mean. The measurement is extremely simple but does require special equipment for measuring the energy (*10*). The crushing energy method is now used routinely in several laboratories.

In a separate experiment, Skidmore et al. (*101, 102*) evaluated abrasive soil loss as influenced by aggregate stability. Soil loss correlated well with the aggregates' resistance to crushing. Log abrasive soil loss was linearly related to aggregate stability (crushing energy method), yielding a coefficient of determination of 0.99.

DRY AGGREGATE SIZE DISTRIBUTION

Tilled surface soils are composed of clods, soil aggregates, and particles of various sizes. The relative amounts of these constituents, on an

air- or oven-dried mass basis, by size class, make up the dry aggregate size distribution (DASD).

The DASD is determined by sieving the dry soil. Early sieving methods used manually or mechanically agitated flat sieves (*29*). Chepil and Bisal (*22*) proposed a standard sieving technique employing a nested set of rotary sieves. The rotary sieve technique has now been generally accepted as the standard technique to determine DASD for wind erosion assessment.

At least once each decade during the past half century, wind erosion researchers have contributed new information on rotary sieves and sieving for determining soil aggregate size distribution and stability. These papers include Chepil and Bisal (*22*), a rotary sieve method; Chepil (*15*), an improved rotary sieve; Chepil (*21*), a compact rotary sieve; Lyles et al. (*77*), a modified rotary sieve; and Fryrear (*39*), a rapid rotary sieve.

Chepil and Bisal (*22*) recommended the rotary sieve over hand sieving mainly because of the wide variance in results obtained among different operators. They attributed this to differences in personal judgment as to the amount of shaking required. Variance between two operators was reduced by using the mechanically operated rotary sieve.

Results obtained by the various models of rotary sieves did not agree well. Lyles et al. (*77*) tested the original, improved, compact, and modified rotary sieves for sieving accuracy with a nonabrasive stone, sand, and gravel mixture and found average errors of 9.4, 32.7, 13.0, and 2.3 percent, respectively. The improved accuracy of the modified rotary sieve was achieved by giving major consideration to mesh length, the primary factor controlling the time sieve material remains on the mesh area.

Even with stable material, size separation by sieving is inherently inaccurate, because of the difficulty of defining unambiguously the point at which to stop the sieving. Part of the difficulty arises because the "near mesh" particles require many encounters with the sieve surface in order to pass through (*51*). With material like soil aggregates, which become abraded or attrited during sieving, not only is defining the end point more difficult but fragile aggregates as from sandy soils may disappear during sieving.

Several alternative methods have been proposed to calculate geometric mean diameter, GMD, and geometric standard deviation, GSD. In his original paper, Gardner (*43*) suggested a graphical approach. Because aggregates are generally log-normally distributed, plots of DASD on log-probability paper, with the log of the sieve diameter as the ordinate, yield straight lines. The GMD is the diameter at 50 percent oversize, and the GSD is calculated as the ratio

$$\text{GSD} = \text{size at 50 percent/size at 15.9 percent} \qquad [4]$$

Gardner (*43*) cautioned that the antilog of GSD has no statistical meaning when determined in this manner.

GMD and GSD also may be calculated from

$$GMD = \exp\left[\sum_{i=1}^{n} m_i \ln d_i\right] = \pi (d_i)^{m_i} \quad [5]$$

$$GSD = \exp\left[\Sigma_{m_i} (\ln d_i)^2 - (\ln GMD)^2\right]^{1/2} \quad [6]$$

where m_i is the mass fraction in each aggregate size class i, d_i is the geometric mean diameter of class i, and π is product operator.

Hagen et al. (*58*) showed that for aggregates that are size distributed log-normally, the mass fraction of aggregates whose diameters are greater or less than some diameter may be represented by use of the error function of the normal distribution curve. This technique requires only two sieve cuts, from which the geometric mean diameter and geometric standard deviation are calculated. Because these two parameters describe the size distribution of log-normally distributed aggregates, the mass fraction of aggregates greater than some user-selected diameter can be calculated easily.

SURFACE ROUGHNESS: SHELTER ANGLE DISTRIBUTION

The importance of soil surface roughness with respect to wind erosion is well documented (*23, 38, 41, 124*). Several surface roughness indices have been developed that summarize cloddiness contributions to surface roughness (*2, 69, 93*), but it has been difficult to apply these indices to wind erosion processes.

Recently, a surface microrelief index was developed based upon a shelter angle concept, the minimum angle from horizontal a particle must descend in order to strike a given location (Figure 12.3) (*87*). The descent angle for a given point was determined by calculating the maximum angle from horizontal between a vertex point and adjacent measured points on the soil surface in a given direction. The angle for a vertex point and an adjacent point was calculated as the arctangent of the ratio between elevation differences and the horizontal distance separating the two points. This procedure was repeated, retaining the same vertex point, for all other points along a transect in a given direction within a 0.3 horizontal distance, termed the influence zone. The maximum angle was retained and defined as the shelter angle, for that individual vertex. This procedure was repeated, incrementing the vertex point and influence zone one point, across the

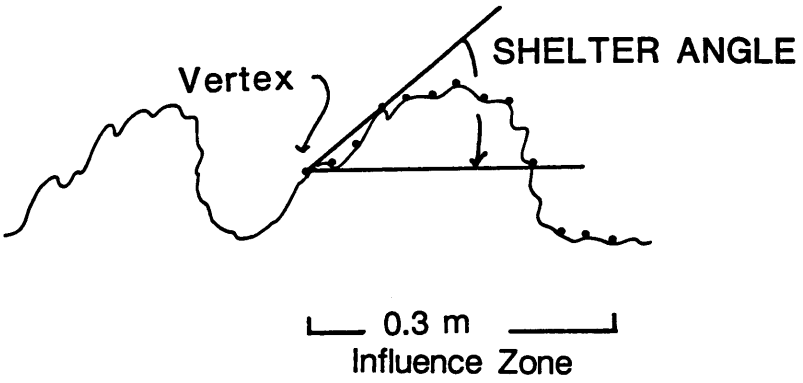

Figure 12.3 Surface roughness schematic illustrating the shelter angle and influence zone concepts (*87*).

transect. Therefore, each measured point has a shelter angle associated with it, except those points near the edge of the plot where the influence zone extended beyond the plot. For points with a negative shelter angle, which indicates that the vertex had a greater elevation than any other point in the influence zone, the shelter angle was set to zero. Therefore, low shelter angles are relatively exposed, so a particle could descend at a very small angle from horizontal and strike the vertex. Large shelter angles would be relatively protected.

The shelter angle for a given vertex represents only that point. To represent the entire surface, many shelter angles are considered by plotting the cumulative shelter angle distribution (CSAD), the fraction of shelter angles less than a given angle versus shelter angle. From the CSAD, the fraction of the measured points with shelter angles equal to or less than an arbitrary angle is easily determined and provides an estimate of the fraction of the surface susceptible to abrasion. In contrast, the fraction of the surface with large shelter angles is likely to be more effective in soil trapping.

Orientation is an important factor for wind erosion control as surface protection, which results from both cloddiness and ridge roughness, varies depending on wind direction relative to the ridge. The effects of ridge and clod roughness can be determined by calculating shelter angles in different directions, i.e., parallel and perpendicular to tillage. An example of shelter angle distributions parallel and perpendicular to sweep tillage with 74-mm ridges is presented in Figure 12.4. It was assumed that the effect of ridging would be minimal in the parallel direction and the CSAD would represent clod roughness. The effect of ridge roughness was determined by calculat-

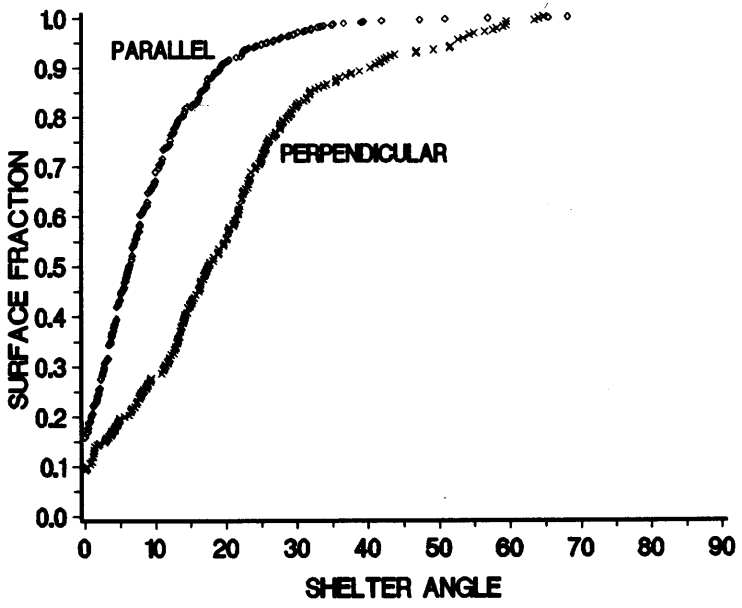

Figure 12.4 Cumulative shelter angle distributions calculated parallel and perpendicular to tillage for a surface with 74-mm ridges (*87*).

ing shelter angles for transects perpendicular to tillage which represents both clod and ridge roughness effects. Therefore, the ridge effect is the difference in the two curves. The fraction of the surface with shelter angles less than 15 degrees for directions parallel and perpendicular to tillage are 80 and 40 percent, respectively.

SURFACE ROUGHNESS: DIGITIZATION OF PIN METER PHOTOS

Parameters that reflect the degree of surface roughness are usually computed from surface elevation measurements. The actual surface elevation data can be obtained through a variety of methods involving image analysis techniques (*90*), microprocessors (*88, 115*), laser systems (*62, 94*), or photography (*119*).

One of the simplest devices to measure surface elevation for calculating shelter angle distribution is a transect, surface profile, pin meter (TSPPM). A typical TSPPM consists of a row of equally spaced pins that contact the soil surface when a measurement is to be taken. The relative

pin elevations are then recorded either manually, electronically, or photographically (Figure 12.5).

Manual recording of field pin elevation data is time consuming and prone to human errors. Electronically recording field elevation data is usually faster and less likely to introduce human-induced errors during the actual recording operation. This is an attractive solution when considering the fact that the elevation data can be stored in digital form in the field. However, automated electronic measurement requires that a data acquisition system, sensors, and power source be available at the measurement site. Therefore, the cost of acquisition, maintenance, and repair must be considered when implementing this type of system, especially when multiple field instruments are necessary. Also, electronic measurement devices may require special instruction and training in the operation and maintenance of the units that may not be possible or feasible.

The third method, photographic techniques, can be as fast as electronic means for recording field pin elevation data, but are less costly and generally do not require special handling and maintenance considerations by the field technician. The disadvantage of photographic techniques is that the data still must be digitized into discrete relative elevation values. This digitization step can be performed either manually or through some automated or semi-automated process.

Recently, a PC-based computer program has been developed (*117*) to automate the digitization of transect, surface profile, pin meter elevation data encoded on photographs (available from USDA-ARS, Wind Erosion Research Unit, Manhattan, KS 66506-4006). The Pin Meter Program (PMP) eliminates the tedious, time-consuming process used in manual digitization methods and reduces the amount of operator judgment required in less automated digitization processes. The PMP is designed to simplify the digitization step and provide more consistent results.

The PMP uses a computer-based hand or page digitization scanner to scan the photograph of a transect, surface profile, pin meter field data. This digitized image is then processed using image analysis techniques to locate the pin edges and thereby compute the pin elevation data. The PMP can then produce the data in the desired format and units as selected by the operator. The data can be displayed on the monitor, printed, and/or stored on disk. This elevation data can then be used to obtain the surface roughness parameters of choice. However, the PMP does require a minimum set of computer hardware and peripherals. Those requirements are

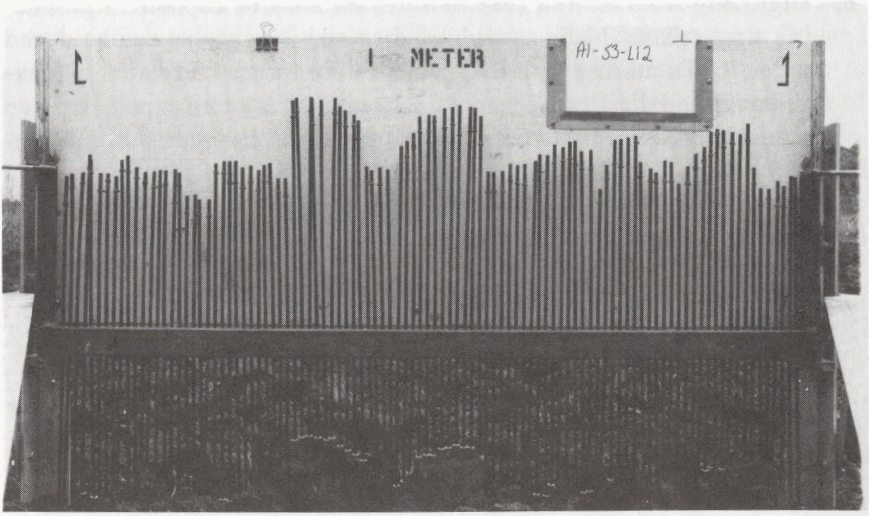

Figure 12.5 Photo of pins in contact with soil surface.

1. An IBM®[1] PC/XT/AT or compatible microcomputer with 640 kilobytes of main memory.
2. MS-DOS or PC-DOS version 2.1 or higher operating system.
3. Additional computer memory supporting the Lotus/Intel/Microsoft (LIM 4.0) Expanded Memory Standard (EMS). Approximately 1.5 megabytes of EMS memory is necessary for a 7.6 by 12.7 cm (3 x 5 in) photo digitized at 300 dpi. The actual amount of EMS memory required is dependent upon the size of the cropped digitized image and the scanner digitizing resolution used.
4. An EGA or VGA graphics adapter with corresponding color monitor is required. Only the 16 color 640 x 350 pixel (EGA) or 640 x 480 pixel (VGA) graphics modes are supported.
5. A Microsoft®[2] compatible mouse with the corresponding software driver.

---

[1] IBM® is a registered trademark of International Business Machines, Inc.
[2] Microsoft® is a registered trademark of Microsoft Corporation.

6. Digitizing scanner. The scanner software must be capable of producing single plane (black and white) digitized images that can be stored in the PC Paintbrush®[3] (.PCX) graphics file format. A relatively inexpensive hand digitizing scanner[4], as compared to more expensive page scanners used during the development of PMP, has provided satisfactory results.
7. A hard disk is not required but highly recommended for convenient storage and retrieval of image and surface profile data files.

Measurement accuracy estimates were made using 20, 101-pin TSPPM photos (3 x 5 in). Each photo was scanned five times at 300 dpi (118 dpts/cm). The standard deviations for the individual pins in each photo were pooled to obtain an estimate of repeatability (standard deviation) of 0.7 mm. This repeatability value may vary with operator, scanner resolution, and contrast quality and size of the TSPPM photos.

SURFACE CRUSTING

Immediately after tillage, the soil surface is usually in a loose, cloddy, unconsolidated condition that is resistant to wind erosion. Heavy rainfall will often produce a consolidated zone at the soil surface, called a surface crust or seal, that is more compact and mechanically stable than some parts of the soil below it (*26*). Soil crusts are generally resistant to erosion by wind alone but they can be rapidly eroded when blowing soil particles are present in the windstream.

Surface crusts have long been the object of scientific investigation, particularly in regard to their effects on plant emergence and water infiltration. Cary and Evans (*13*) have presented an excellent review of crust formation and management. A review of the effects of crust formation on crop establishment has been presented by Awadhwal and Thierstein (*5*). A recent international symposium on surface crusting included sessions on the genesis and morphology of crusts; effects of crusts on seedling emergence, water and gas transfer, and water erosion; methodology to characterize crusts; and crust management (*12*). Few studies have considered the effects of surface crusts on wind erosion.

---

[3]PC Paintbrush® is a registered trademark of Zsoft Corporation.

[4] The actual hand scanner used was DFI Handy Scanner model HS-3000 by Diamond Flower Electric Instrument Co., (USA) Inc., 2455 Port Street, West Sacramento, CA 95961, USA. The use of trade names in this publication does not imply endorsement of the products named.

When crusts are present, the mechanically more stable crust is less susceptible to abrasion by blowing soil than the soil beneath the crust. Crusted soils have been found to erode at a rate of approximately one-sixth to one-half the rate of uncrusted soil (*19*). A determination of the ability of crusts to withstand the abrasive action of blowing soil, the abrasive resistance, is an important factor in the characterization of soil crusts for wind erosion assessment. Crust abrasive resistance has been measured in the laboratory (*14, 33, 126, 127*) and in the field (*24, 28*) using wind tunnel tests.

We describe a common laboratory procedure employed to measure crust abrasive resistance. The procedure requires a rainfall simulator and wind tunnel. Soils are placed in trays approximately 5 cm deep, 30 cm wide, and 100 to 150 cm long. The trays are then subjected to simulated rainfall to create a crusted condition and air-dried or oven-dried at approximately 50°C to simulate field conditions. The bottoms of the trays are perforated to allow water movement through the soil. The trays are then placed in a wind tunnel and abraded using natural aeolian sand or sieved sandy soil. Abrader that is composed of sieved soil material should include portions of the fine and/or medium sand fractions, 100 to 500 um in diameter. Abrader is introduced onto the floor of the wind tunnel using an abrader feeding device that drops a known amount of abrader on the floor of the tunnel through a calibrated orifice. The abrader rapidly reaches maximum velocity using this procedure.

Alternatively, a known amount of abrader can be simply placed on the floor on the up-wind end of the wind tunnel. The latter procedure is suggested only in relatively long wind tunnels, where the initially motionless abrader has time to reach maximum velocity before striking the crusted soil surface. The trays of crusted soil are initially weighed, abraded, and reweighed. The soil loss (mass per unit area) is computed as the difference in tray weight.

In general, the cumulative tray soil loss is linearly related to the cumulative amount of abrader that has passed over the crust. Typical abrasion curves for three crusted soils are illustrated in Figure 12.6. The coefficient of abrasion is calculated from these data by relating the cumulative amount of tray soil loss, as the dependent variable, to the cumulative amount of abrader passing over the crusted soil, as the independent variable, using linear regression analysis. The slope of the line is the coefficient of abrasion. Departures from straight line trends indicate that the amount of abrasion is changing through time, which is often caused by partial destruction of the crusted surface (*14*) or gradient in abrasive resistance of consolidated zone.

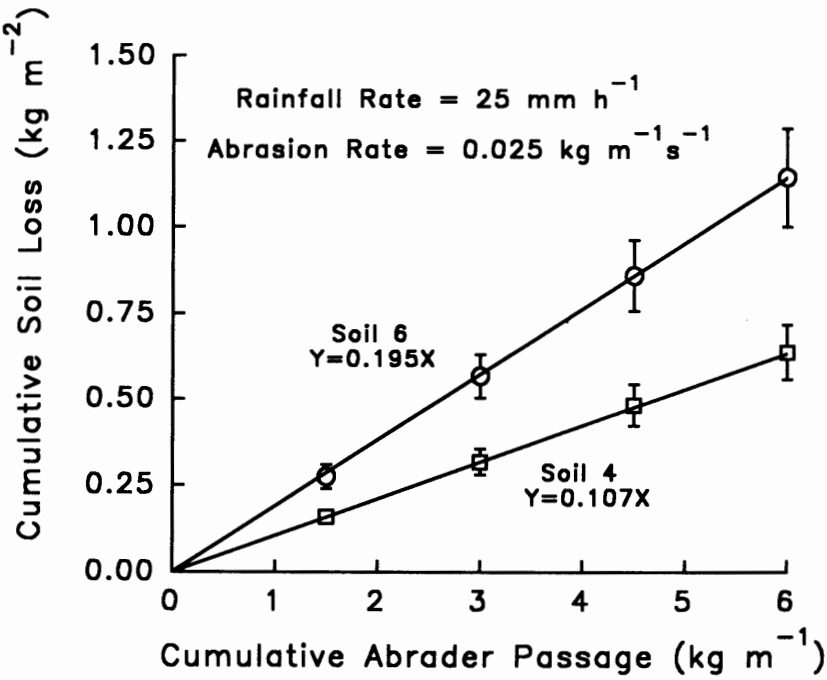

Figure 12.6 Relation of cumulative soil loss and cumulative abrader passage (*127*).

LOOSE SURFACE PARTICLES

Loose particles on a weakly crusted surface are easily eroded by wind. They impact significantly on initiation and perpetuation of wind erosion. Particles between 0.1 and 0.5 mm are easily moved by wind in saltation. The impact force of saltating particles on the soil surface dislodges other soil particles and abrades large soil aggregates into an erodible size (*52*). Chepil (*19*) discussed the interactive relationship between crust strength and abrader quantity on wind erosion. Soils that develop strong crusts, a surface "armor", with little loose abrader material present on the surface are resistant to wind erosion. Other soils that form weak crusts erode readily even though relatively small amounts of abrader are present initially.

Loose material may be generated by a number of mechanisms other than direct abrasion, including freeze-thaw, freeze-dry, and rainfall. We describe here a vacuum method to measure the amount of loose material resting on a crusted surface after a rainfall event. The system had two sedimentation chambers or separators with a combined efficiency of 90 percent (Figure 12.7). The first separator was a modified army ammuni-

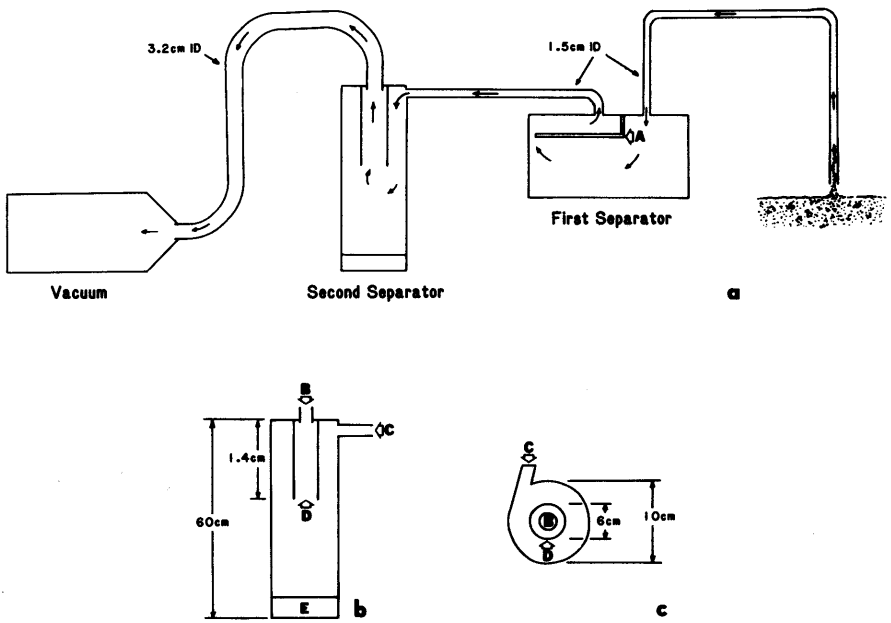

Figure 12.7 Schematic of the vacuum collection system used to collect loose materials. (a) Cross section of the entire system; (b) detail of vertical cross section of the second separator (A—air outlet, B—air inlet, C—tubular guard, and D—bottom cap); (c) detail of horizontal cross section of the second separator (*126*).

tion can with an L-shaped baffle that separated the intake and outflow tubes. The first separator retained most of the sample, allowing relatively clean air to enter the top of the second separator. The second separator was a conventional reverse-flow cyclone with a cylindrical tubular guard that extended below the level of the air outlet to restrict sediment movement. The sample was collected by removing the bottom cap (Figure 12.7). The vacuum was generated by a light-weight vacuum cleaner (110V AC; 1.0 peak horse power motor) powered by a portable generator. Because the surface was not brushed or disturbed during the vacuuming process, the material collected was loose on the soil surface.

Potter (*86*) used this system to develop functions relating quantity of loose particles on the soil crusts after a rainfall event to amount of rain and percent sand in the soil. He found that the variability among soils was large. Coefficients of variation (CV) ranged from 9 to 124 percent and were generally as large or larger for the finer textured soils as for the coarser textured soils. Soil texture had the greatest influence on the amount of loose material on the crusted soil surface. The quantity of loose material

was small for the finely textured soils, but increased rapidly as sand content increased. About 30 times as much loose material occurred on the coarsest textured soil (0.091 kg m^{-2}) compared to the finest textured soil (0.003 kg m^{-2}) in Potter's (*86*) study. The vacuum collection system worked satisfactorily to sample loose granular materials on the crusts of the soils tested.

SOIL WETNESS

Soil wetness, particularly at the soil-atmosphere interface, greatly influences soil erodibility by wind. Therefore, an accurate evaluation of soil wetness is a prerequisite for any reliable wind erosion prediction scheme. Chepil (*17*) showed that the resistance of the uppermost soil particles against wind erosion, on the average, was proportional to the equivalent soil water content squared, when equivalent water content was defined as the ratio of the amount of water held in the soil to the amount held by the same soil at -1500 Joules/Kg soil water potential. This was the basis for developing a climatic factor in the wind erosion equation used to predict the amount of soil that will erode from a given agricultural field and to determine the conditions necessary to reduce potential erosion to a tolerable amount (*27*).

The water content at the interface of the soil and the atmosphere is constantly changing. It may change rapidly because of rainfall, irrigation, and/or hail, or slowly because of evaporation, drainage, and in the form of dew or soft-landing snowflakes. The water thus received at the soil surface may run off or infiltrate into the soil and be distributed in the soil volume according to the laws that govern saturated and unsaturated moisture flow, or it may evaporate from the surface.

When the evaporation rate from the soil exceeds the soil's ability to transmit water to that surface, the amount of water in the surface soil can change rapidly. Idso et al. (*63*), using albedo measurements, found that surface volumetric water of a bare Avondale loam soil at Phoenix, Arizona, decreased from 0.20 to 0.07 cm^3/cm^3 between 1300 and 1500 h two days after the soil was irrigated in July. This process was slower in December when the surface soil did not dry until 10 days after irrigation; the volumetric water content decreased from 0.16 to 0.06 cm^3/cm^3 between 1000 and 1500 h. This is significant considering that the amount of water retained at -1500 Joules/Kg water potential for the Avondale loam is 0.15 m^3/m^3 which indicates the soil surface can attain wind-erodible dryness in a few hours.

Van Bavel and Hillel (*113*) presented a dynamic simulation model for calculating the water content and temperature profiles of a bare soil with

global radiation, wind speed, air temperature, and dew point temperatures as the only time-dependent input data. Their model can simulate the simultaneous flow of heat and water in a vertical soil profile.

Hillel (*59*), in Computer Simulation of Soil-Water Dynamics, described the formulation of several models simulating soil physical processes. One of these, the model for nonisothermal evaporation of soil water, was modified by Skidmore and Dahl (*100*) to examine the behavior of surface-soil drying as influenced by atmospheric evaporativity, soil hydraulic properties, and initial water content. They examined soil-water dynamics of the surface cm of soil as influenced by evaporativity, soil hydraulic properties, and initial water content. Diurnal wind speed, global irradiance, and air and dew point temperatures for selected days were used to calculate nonisothermal evaporation from hypothetical clay, loam, and sand soil. Surface soil dried quickly to wind-erodible dryness (-1500 joules/kg), especially for meteorological conditions conducive to wind erosion. When the soil was wet (-10 joules/kg) and the weather was typified by medium-high irradiance and strong winds, sand, loam, and clay soils dried to wind-erodible dryness by the first, second, and third days, respectively. When the soil was somewhat drier (-100 joules/kg) initially, it dried to wind-erodible dryness in a few hours. The quick drying of bare surface soil must be considered in the study of the processes that occur at or near the surface.

Lascano and van Bavel (*70, 71*) verified a similar model on bare soil. Using soil hydraulic properties and standard meteorological data as input, their calculated profiles compared favorably to actual measurements. The predicted water content values were within one standard deviation of the average measured values. Bristow et al. (*11*) added a residue component to model dynamic aspects of mass and energy transfer in a soil-residue-atmosphere system.

Although the simulation models that have been developed recently seem to be capable of predicting water content profiles, most require detailed information about soil hydraulic properties and much computer time—maybe more than feasible for the wind erosion modeling. Furthermore, these models fail to predict soil wetness at the soil-atmosphere interface which can be significantly different from that below the surface.

Both Chepil et al. (*27*) and Skidmore (*98*) have assumed that on a long-term basis, equivalent surface water content was approximated by the ratio of precipitation to potential evaporation. If effective precipitation exceeds potential evaporation, the soil remains wet. On the other hand, if potential evaporation far exceeds precipitation, the soil surface must be dry most of the time.

Another estimator of soil wetness is the ratio of actual evaporation to potential evaporation. Water will evaporate from the soil surface at the potential rate only when the surface is wet. When the soil cannot supply water to the surface fast enough to keep up with potential evaporation rate, the surface dries, and the evaporation rate declines below the potential rate. When actual evaporation rate is very slow compared to the potential rate, the surface must be dry. Therefore, the ratio of actual evaporation to potential evaporation is an indicator of the dryness of the soil surface.

To meet the unique requirements of wind erosion prediction technology, a computer simulation of soil water dynamics is being developed and validated for the HYDROLOGY submodel of the Wind Erosion Research Model (*34*).

The HYDROLOGY submodel maintains a continuous soil water balance by accounting for daily amounts of infiltration, snow melt, soil evaporation, plant transpiration, runoff, and deep percolation. The potential evapotranspiration, which is calculated by a combination equation, is partitioned between bare soil evaporation and plant transpiration on the basis of plant leaf area index. Additionally, soil water redistribution by water flow up and down between soil layers is evaluated on an hourly basis using Darcy's flow equation. The first objective of the HYDROLOGY submodel is to estimate water contents of the different soil layers. Potential rates of soil evaporation and plant transpiration are adjusted to actual rates on the basis of soil water availability. Deep percolation from the soil profile is estimated to be equal to the conductivity of the lowermost soil layer, assuming a unit hydraulic gradient at the lower boundary.

Furthermore, the unique feature of this submodel is its ability to estimate soil wetness at the soil-atmosphere interface on an hourly basis as needed by the EROSION submodel. This is accomplished by extrapolating water content from the three uppermost simulation layers, using a second order polynomial equation, and by interpolating the relationship between the evaporation ratio and equivalent surface soil water content.

The submodel was originally tested using the soil water and climatic data from a 1971 bare soil evaporation experiment conducted on an Avondale loam (fine-loamy, mixed [calcareous], hyperthermic Typic Torrifluvent) at the U.S. Water Conservation Laboratory, Phoenix, Arizona (*65*). Further testing was conducted during July-August 1991 on a Pullman clay loam (fine, mixed, thermic Torrertic Paleustoll) at the USDA-ARS Conservation and Production Research Laboratory at Bushland, Texas.

The simulated evaporation results agreed well with the measured daily evaporation rates from lysimeters during the duration of the two experiments. Furthermore, the submodel reasonably estimated the soil water

content profiles, particularly soil wetness at the soil-atmospehre interface as compared with measured water contents from the uppermost 2 and 5 millimeters of the soil in the Texas and Arizona experiments, respectively.

Based on our limited testing, the HYDROLOGY submodel is adequate in predicting soil wetness as needed for wind erosion modeling.

CANOPY STRUCTURE

Plant growth simulation models range from the relatively simple, such as SUCROS (*114*), to the extremely complex process-orientated SIMCOTT II (*81*) and from the universal models that simulate many different plants, such as EPIC (*123*), to models that simulate the growth of only one particular species (*3, 60, 67, 117*) or only a specific plant part (*61*). The one common characteristic of all these models is the main output, which is dry weight of the biomass produced. Dry weight is often required in soil erosion modeling.

Canopy structure characteristics of height, structure and flexibility of individual plants, size and arrangement of plant parts, and the number of plants occupying a given area determine its aerodynamic roughness, thus affecting the friction velocity at the top of the canopy (*96*). The distribution of leaf and stem area with height is needed to determine the depletion of the friction velocity through the plant canopy and, thus, the velocity near the soil surface (*6*). Distinguishing between stem and leaf area is necessary because leaves tend to streamline with the wind flow and have a drag coefficient (C_d) of about 0.1, whereas stems remain rigid and have a C_d of about 1.0. Thus, on a unit area basis, stems are about 10 times more effective than leaves in depleting the friction velocity.

Following is an approach used by Armbrust and Bilbro (*4*) for predicting canopy structure.

Thirty plants were sampled every seven days from emergence to maturity. Plants were cut at the soil surface, placed in sealed plastic bags with wet paper towels, and returned to the laboratory where the following measurements were made:

1. Plant height—base of plant to top leaf curve or top of head.
2. Stem length—base of plant to top leaf collar.
3. Stem diameter—2 cm above base and at top leaf collar, including sheath.
4. Peduncle length—above top leaf collar to bottom of head.
5. Peduncle diameter—above top leaf collar and at bottom of head.
6. Length and width of head, if present—width at midpoint of length.

7. Dry weight of head—only that part of head emerged from leaf sheath.
8. Dry weight of sections of stems and leaves equal to one-fifth of plant height and leaf area of each section.

Canopy cover was measured weekly at solar noon (1134 CDT + or - 1 hr) in the field on three areas, each 2 m by 0.76 m, selected immediately after planting, and five positions in each area were marked as locations for canopy cover determination by the meter stick method (*1*).

Armbrust and Bilbro (4) fit equations to the natural growth function equation

$$Y = a\left(1 - e^{bx}\right) \qquad [7]$$

where Y = parameter to be estimated, X = total above-ground dry weight, a = asymptotic value of Y, and b = rate at which Y approaches "a" for several crops. They found that stem area of grain sorghum remained in the bottom 80 percent of the plant height. Average leaf and stem areas versus normalized height is shown in Figure 12.8.

FIELD SCALE WIND EROSION MEASUREMENT

Wind erosion has proven difficult to measure in the field. Attempts have been made to measure change in soil depth resulting from wind erosion (*26, 45*). A change in soil depth of 1.0 mm for a one-year period represents excessive wind erosion on many soils and contributes a significant load to the atmospheric aerosol. It is difficult to measure even 1.0 mm change in depth because the surface is rough and the elevation of the soil is not constant. It may vary several mm because of change in water content or change in bulk density resulting from tillage or compaction.

Redistribution of the fallout radionuclide cesium-137 has been used to estimate net sediment redistribution from wind erosion (*111*). This technique is also limited to long-term studies. Long-term trends in erosion, although useful, do not provide detailed information about wind erosion processes. To investigate erosion processes, measurements encompassing a single storm are needed, or even better, measurements of erosion continuously within the storm event.

Various techniques have been used to measure short-term wind erosion. These include columns of cake-pans and psammagraphs (*32*); tipping-bucket gauge (*80*); vertical tube sand traps (*72*); adhesive tape (Mainquet, Reims, France, personal communication); and numerous vertical slot samples (*7, 18, 82*). Fryrear et al. (*42*) outlined equipment and procedure for measuring field erosion.

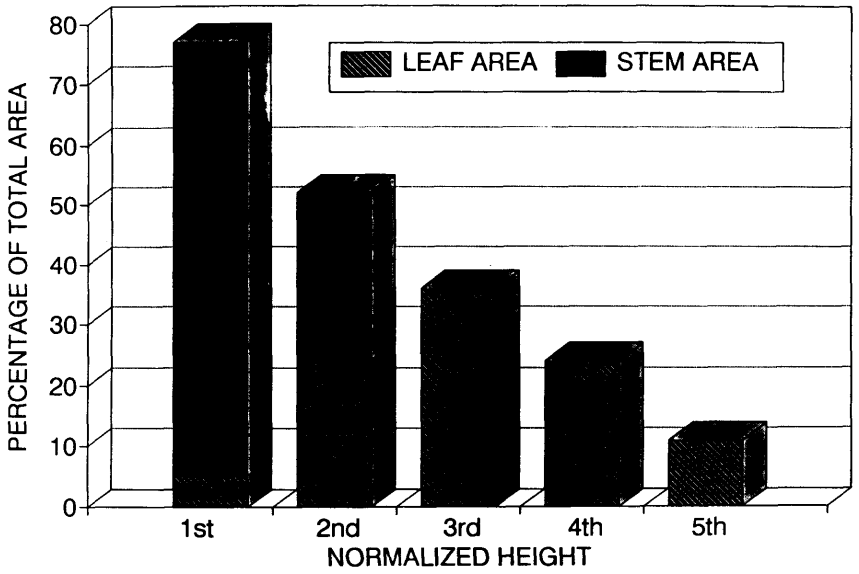

Figure 12.8 Grain sorghum leaf and stem area distribution with normalized plant height. Average for all sample dates from emergence to maximum canopy cover.

Creep and saltation

Because wind eroded soil is transported in various modes, field instruments must be designed to provide samples of eroding soil in the separate transport modes. The creep component of the soil flux can be sampled using an exposed horizontal slot or circular opening that leads to a buried container. If a slot is used, it should be able to rotate so it remains normal to the wind direction. The important consideration is to avoid surface protuberances that prevent the sampler from collecting a representative sample of the moving soil. A small fraction of saltation flux is also trapped by creep samplers, but this can be estimated by sieving the trapped sample.

Vertical slot samplers are generally used for trapping saltating particles. Their overall efficiency is the product of the entrance efficiency and the trapping efficiency for particles that have passed the entrance. An early slot sampler was developed by Bagnold (*7*), but it did not rotate into the wind. Tests on a slot sampler similar to Bagnold's showed it was only about 60 percent efficient (*48*). Chepil (*18*) modified Bagnold's sampler to rotate into the wind. Later, trapping efficiency was improved by venting catchers (*37*) and also by making the sampler in a wedge shape to increase the area for air flow between the inlet slot and the vents (*82*).

Stout and Fryrear (*110*) developed an improved slot sampler for saltation and creep particles. Features of the improved sampler included a vented, wedge-shaped inlet section that was 98 percent efficient for trapping saltation in tunnel tests. In addition, the base at the soil surface consisted of a nonrotating outer portion and a rotating inner portion, so that the rotating portion could not contact the soil surface as in earlier samplers. Because the sampler is 0.2 m tall, it must be combined with other samplers to completely sample the saltation zone. Stout's sampler is currently being used in the WEPS field studies.

Suspension

Accurate sampling of suspended particles requires an isokinetic sampler, i.e., one in which inlet velocity and surrounding air velocity are equal. Sampling errors caused by nonisokinetic sampling depend on both particle size and level of deviation from isokinetic flow (*31*). To achieve near-isokinetic sampling, horizontal inlet tubes coupled to a filter and powered suction device have been used (*25, 47*). Steen (*109*) developed a passive sampler shaped as a diffuser to induce isokinetic inlet flow, but then used power to provide electrostatic trapping of the particles. In general, these samplers were not suitable for untended operation near the surface in an eroding field where high particle concentrations are the norm. Fryrear (*40*) developed a low-cost, wedge-shaped, passive sampler that rotates into the wind, dubbed the BSNE. The sampler provides near-isokinetic inlet conditions and separates particles from the flow by using a combination of particle settling, impact, and a screened outlet. The BSNE sampler efficiency averaged over 89 percent on samples of washed sand and sieved soil. For particles less than 0.050 mm diameter, the efficiency decreased. However, trapped samples can be sieved and mathematically adjusted to account for effects of known trapping efficiencies. A combination of Stout and BSNE samplers allows measurement of soil flux profiles from the surface to a height of several meters.

Threshold

Most wind erosion models require an accurate estimate of threshold conditions and erosion duration during field tests. Thus, a method to determine both the onset and cessation of saltation is needed. To accomplish this task, a piezoelectric quartz crystal impact sensor has been developed for field use (*48*). The sensor, called SENSIT, counts particle impacts at a fixed height near the surface. Coupled with wind speed and direction sensors, SENSIT allows onset, duration, and direction of wind erosion to be monitored.

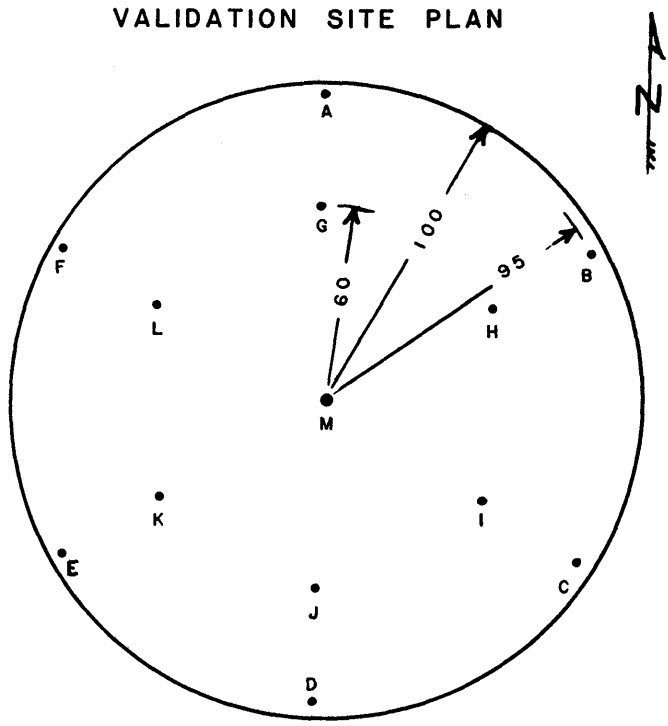

Figure 12.9 Plan for locating 14 clusters (A through N) of samplers in a 200-meter diameter circular field.

Field installation

For a typical uniform field with a well defined non-eroding boundary, the following equipment and instruments were used by Fryrear et al. (*42*).

Meteorological tower instrumented with the following

- four anemometers, 0.20, 0.50, 1.0, and 2.0 m
- two air temperatures, 0.2 and 2.0 m
- one solar radiation
- one soil temperature, 0.02 m
- one wind direction, 2.5 m
- one tipping bucket rain gauge
- one relative humidity sensor, 2.0 m

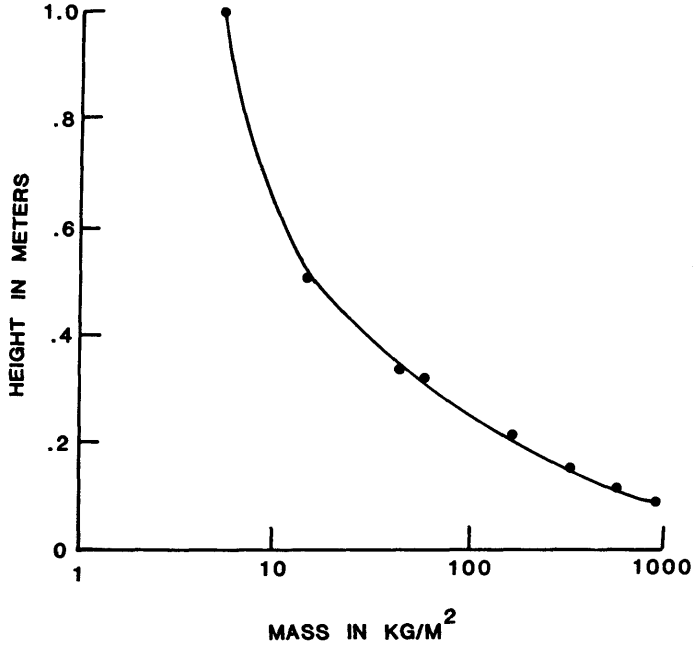

Figure 12.10 Vertical distribution of airborne mass to a height of 1 meter on March 11, 1988, 134 meters from an upwind non-eroding surface at Big Spring, Texas.

Erosion samplers

- 14 clusters BSNE samplers at 0.05, 0.10, 0.20, 0.5, and 1.0 m above the soil surface (located as illustrated in Figure 12.9)
- one surface creep (0.0 to 0.003 m height, 0.005 m wide opening) with saltation (0.003 to 0.02)
- one weighing BSNE sampler at 0.02 m height
- one SENSIT (threshold) at 0.02 m height

This array and selection of samplers enabled one technician to maintain a site. After every dust storm, all samplers were emptied, the contents were transferred to metal containers, and temporal soil field conditions that had changed since the last measurements were recorded. Typical vertical and horizontal distributions of eroded material collected in the above described arrangement of samples are shown in Figures 12.10 and 12.11.

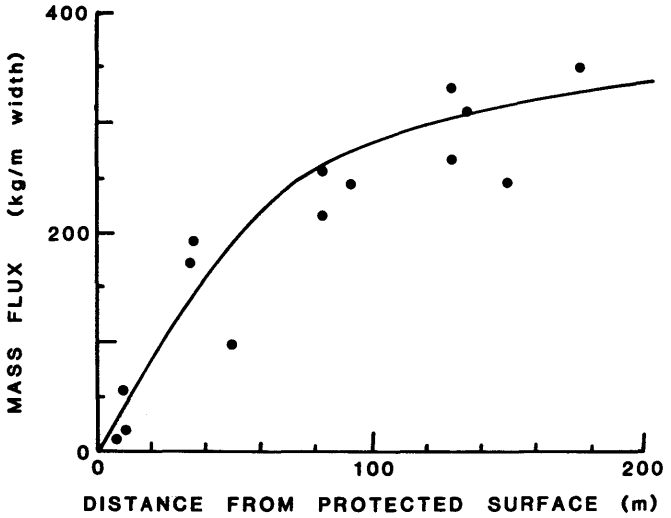

Figure 12.11 Horizontal distribution of eroded mass across a 200-meter-wide field at Big Spring, Texas, March 11, 1988.

REFERENCES

1. Adams, J.E., and G.F. Arkin. 1977. *A light interception method for measuring row crop ground cover.* Soil Science Society of America Journal 41: 789-792.
2. Allmaras, R.R., R.E. Burwell, W.E. Larson, and R.F. Holt. 1966. *Total porosity and random roughness of the interrow zone as influenced by tillage.* Conservation Research Report 7. U.S. Department of Agriculture. 22 pp.
3. Arkin, G.F., R.L. Vanderlip, and J.T. Ritchie. 1976. *A dynamic grain sorghum growth model.* Transactions, American Society of Agricultural Engineers 19: 622-626, 630.
4. Armbrust, D.V., and J.D. Bilbro. 1988. *Prediction of canopy structure for wind erosion modeling.* Paper No. 88-2559, International Winter Meeting, American Society of Agricultural Engineers, December 13-16, Chicago, Illinois.
5. Awadhwal, N.K., and G.E. Thierstein. 1985. *Soil crust and its impact on crop establishment: A review.* Soil Tillage Research 5: 289-302.
6. Bache, D.H. 1986. *Momentum transfer to plant canopies: influence of structure and variable drag.* Atmosphere and Environment 20: 1369-1378.
7. Bagnold, R.A. 1943. *The physics of blown sand and desert dunes.* London, Methuen, 265.
8. Barndorff-Nielsen, O.E., J.L. Sensen, H.L. Nielsen, K.R. Rasmussen, and M. Sorensen. 1985. *Wind tunnel tracer studies of grain progress.* Proceedings, International Workshop on Physics of Blown Sand. Department of Theoretical Statistics, University of Aarhus, Aarhus, Denmark. 2: 243-252

9. Bondy, E., L. Lyles, and W.A. Hayes. 1980. *Computing soil erosion by periods using wind energy distribution.* Journal of Soil and Water Conservation 35: 173-176.
10. Boyd, D.W., E.L. Skidmore, and J.G. Thompson. 1983. *A soil-aggregate crushing-energy meter.* Soil Science Society of America Journal 47: 313-316.
11. Bristow, K.L., G.S. Campbell, R.J. Papendick, and L.F. Elliott. 1986. *Simulation of heat and moisture transfer through a surface residue-soil system.* Agriculture and Forest Meteorology 36: 193-214.
12. Callebaut, F., D. Gabriels, and M. DeBoodt. 1986. *Assessment of soil surface sealing and crusting.* Proceedings, Symposium in Ghent, Belgium, 1985. State University of Ghent.
13. Cary, J.W., and D.D. Evans (eds.). 1974. *Soil crusts.* University of Arizona Agricultural Experiment Station Technical Bulletin 214. Tucson.
14. Chepil, W.S. 1951. *Properties of soil which influence wind erosion: V. Mechanical stability of structure.* Soil Science 72: 465-478.
15. Chepil, W.S. 1952. *Improved rotary sieve for measuring state and stability of dry soil structure.* Soil Science Society of America Proceedings 16: 113-117.
16. Chepil, W.S. 1953. *Field structure of cultivated soils with special reference to erodibility by wind.* Soil Science Society of America Proceedings 17: 185-190.
17. Chepil, W.S. 1956. *Influence of moisture on erodibility of soil by wind.* Soil Science Society of America Proceedings 20: 288-292.
18. Chepil, W.S. 1957. *Width of field strips to control wind erosion.* Kansas Agricultural Experiment Station Technical Bulletin 92. p. 16.
19. Chepil, W.S. 1958. *Soil conditions that influence wind erosion.* U.S. Department of Agriculture, Agricultural Research Service Technical Bulletin 1185. U.S. Government Printing Office, Washington, D.C.
20. Chepil, W.S. 1960. *Conversion of relative field erodibility to annual soil loss by wind.* Soil Science Society of America Proceedings 24: 143-145.
21. Chepil, W.S. 1962. *A compact rotary sieve and the importance of dry sieving in physical soil analysis.* Soil Science Society of America Proceedings 26: 4-6.
22. Chepil, W.S., and F. Bisal. 1943. *A rotary sieve method for determining the size distribution of soil clods.* Soil Science 56: 95-100.
23. Chepil, W.S., and R.A. Milne. 1941. *Wind erosion of soils in relation to the size and nature of the exposed area.* Sci. Agric. 21: 479-487.
24. Chepil, W.S., and N.P. Woodruff. 1954. *Estimations of wind erodibility of field surfaces.* Journal of Soil and Water Conservation 9: 257-265.
25. Chepil, W.S., and N.P. Woodruff. 1957. *Sedimentary characteristics of dust storms: II. Visibility and dust concentration.* American Journal of Science 255: 104-114.
26. Chepil, W.S., and N.P. Woodruff. 1963. *The physics of wind erosion and its control.* Advances in Agronomy 15: 211-302.

27. Chepil, W.S., F.H. Siddoway, and D.V. Armbrust. 1962. *Climate factor for estimating wind erodibility of farm fields.* Journal of Soil and Water Conservation 17: 162-165.
28. Chepil, W.S., N.P. Woodruff, and A.W. Zingg. 1955. *Field study of wind erosion in western Texas.* U.S. Department of Agriculture Technical Bulletin SCS-TP-125.
29. Cole, R.C. 1939. *Soil macrostructure as affected by cultural treatments.* Hilgardia 12: 429-472.
30. Coleman, N.L., and W.M. Ellis. 1976. *Model study of the drag coefficient of a streambed particle.* Proceedings 3rd Federal Interagency Sedimentation Conference, March 22-25, Denver, Colorado.
31. Davies, C.N. 1968. *The entry of aerosols into sampling tubes and heads.* British Journal of Applied Physics Ser. 2. (1): 921-923.
32. DePloey, J. 1980. *Some field measurements and experimental data on windblown sands.* In: M. DeBoodt and D. Gabriels (eds.) *Assessment of erosion.* John Wiley and Sons. pp. 541-553.
33. Diouf, B., E.L. Skidmore, J.B. Layton, and L.J. Hagen. 1990. *Stabilizing fine sand by adding clay: Laboratory wind tunnel study.* Soil Tech. 3: 21-31.
34. Durar, A.A., and E.L. Skidmore. 1989. *The hydrologic components of the wind erosion research model.* Agronomy Abstracts. Madison, Wisconsin. p. 278.
35. Elliot, D.L., C.G. Holladay, W.R. Barchet, H.P. Foote, and W.F. Sandusky. 1987. *Wind energy resource atlas of the United States.* DOE/CH 10093-4. Available from National Technical Information Service, Springfield, Virginia.
36. Farrell, D.A., E.L. Greacen, and W.E. Larson. 1967. *The effect of water content on axial strain in a loam soil under tension and compression.* Soil Science Society of America Proceedings 31: 445-450.
37. Fryberger, S.G., T.S. Ahlbrandt, and S. Andrews. 1979. *Origin, sedimentary features, and significance of low-angle aeolian "sand sheet" deposits, Great Sand Dunes, National Monument and vicinity, Colorado.* Journal of Sedimentary Petrol. 49(3): 733-746.
38. Fryrear, D.W. 1984. *Soil ridges-clods and wind erosion.* Transactions, American Society of Agricultural Engineers 18: 445-448.
39. Fryrear, D.W. 1985. *Determining soil aggregate stability with a rapid rotary sieve.* Journal of Soil and Water Conservation 40: 231-233.
40. Fryrear, D.W. 1986. *A field dust sampler.* Journal of Soil and Water Conservation 41(2): 117-120.
41. Fryrear, D.W., and E.L. Skidmore. 1985. *Methods of controlling wind erosion.* In: R.F. Follett and B.A. Stewart (eds.) *Soil Erosion and Crop Productivity.* American Society of Agronomy, Crop Science Society of America, Soil Science Society of America, Madison, Wisconsin. p. 443-457.
42. Fryrear, D.W., J.E. Stout, L.J. Hagen, and E.D. Vories. 1990. *Wind erosion: field measurement and analysis.* Transactions, American Society of Agricultural Engineers 3: 155-160.

43. Gardner, W.R. 1956. *Representation of soil aggregate-size distribution by a logarithmic-normal distribution.* Soil Science Society of America Proceedings 20: 151-153.
44. Gerety, K.M., and R. Slingerland. 1983. *Nature of the saltating population in wind tunnel experiments with heterogeneous size-density sands.* In: M.E. Brookfield and T.S. Ahlbrant (eds.) *Developments in Sedimentology* 38: 115-151, Elsevier, New York.
45. Gibbens, R.P., J.M. Tromble, J.T. Hennessy, and M. Cardenas. 1983. *Soil movement in mesquite dunelands and former grasslands of southern New Mexico from 1939 to 1980.* Journal of Range Management 36: 145-148.
46. Gill, W.R., and W.F. McCreery. 1960. *Relation of size of cut to tillage tool efficiency.* Agricultural Engineering 41: 372-374, 381.
47. Gillette, D.A., I.H. Blifford, and C.R. Fenster. 1972. *Measurements of aerosol size distributions and vertical fluxes of aerosols on land subject to wind erosion.* Journal of Applied Meteorology 11: 977-987.
48. Gillette, D.A., and P.H. Stockton. 1986. *Mass momentum and kinetic energy fluxes of saltating particles.* In: William G. Nickling, (ed.) *Aeolian Geomorphology.* Allen and Unwin, Boston, pp. 35-56.
49. Greeley, R., and J.D. Iversen. 1985. *Wind as a Geological Process.* Cambridge University Press, Cambridge.
50. Grossman, R.B., J.B. Fehrenbacker, and A.H. Beavers. 1959. *Fragipan soils of Illinois: I. General characterization and field relationships of Hosmer silt loam.* Soil Science Society of America Proceedings 23: 65-70.
51. Gupta, V.S., D.W. Fuerstenau, and T.S. Mika. 1975. *An investigation of sieving in the presence of attrition.* Power Technology 11: 257-271.
52. Hagen, L.J. 1984. *Soil aggregate abrasion by impacting sand and soil particles.* Transactions, American Society of Agricultural Engineers 27: 805-816.
53. Hagen, L.J. 1988. *New wind erosion model developments in the U.S. Department of Agriculture.* Proceedings of the 1988 Wind Erosion Conference. Texas Tech. University, Lubbock. pp. 104-116.
54. Hagen, L.J. 1991. *Wind erosion mechanics: Abrasion of aggregated soil.* American Society of Agricultural Engineers 34(4): 891-837.
55. Hagen, L.J. 1991. *A wind erosion prediction system to meet user needs.* J. Soil and Water Conserv. 46: 105-111.
56. Hagen, L.J., and D.V. Armbrust. 1989. *Aerodynamic roughness and saltation trapping efficiency of tillage ridges.* Transactions, American Society of Agricultural Engineers 35: 1179-1184.
57. Hagen, L.J., L. Lyles, and E.L. Skidmore. 1980. *Application of wind energy to Great Plains irrigation pumping.* Advances in Agricultural Technology, USDA-AAT-NCO-4, 20 pp.
58. Hagen, L.J., E.L. Skidmore, and D.W. Fryrear. 1987. *Using two sieves to characterize dry soil aggregate size distribution.* Transactions, American Society of Agricultural Engineers 30: 162-165.
59. Hillel, D. 1977. *Computer simulation of soil-water dynamics.* International Development Research Center, Ottawa, Canada, 214 pp.

60. Holt, D.A., R.J. Bula, G.E. Miles, M.M. Schreiber, and R.M. Peart. 1975. *Environmental physiology, modeling, and simulation of alfalfa growth. I. Conceptual development of SIMED.* Purdue University Agricultural Experiment Station Research Bulletin No. 907. Lafayette, Indiana.
61. Hoogenboom, G., and M.G. Huck. 1986. *ROOTSIMU V4.0: A dynamic simulation of root growth, water uptake, and biomass partitioning in a soil-plant-atmosphere continuum: update and documentation.* Alabama Agricultural Experiment Station Agronomy and Soils Department Series No. 109, 84 pp.
62. Huang, C., I. White, E.G. Thwaite, and A. Bendeli. 1988. *A noncontact laser system for measuring soil surface topography.* Soil Science Society of America Journal 52: 350-355.
63. Idso, S.B., R.D. Jackson, R.J. Reginato, B.A. Kimball, and F.J. Nakayama. 1975. *The dependence of bare soil albedo on soil water content.* Journal of Applied Meteorology 14: 109-113.
64. Iverson, J.D. 1986. *Small scale wind tunnel modeling of particle transport—Froude number effect.* Aeolian Geomorphology 19-33.
65. Jackson, R.D. 1973. *Diurnal changes in soil water content during drying.* In: *Field Soil Water Regime.* Soil Science Society of America Special Publication No. 5, pp. 37-55.
66. Jensen, M. 1958. *The model-law for phenomena in natural wind.* Ingenioren 2: 121-128.
67. Johnson, I.R., T.E. Ameziane, and J.H.M. Thornley. 1983. *A model of grass growth.* Ann. Bot. 51: 599-609.
68. Kind, R.J. 1976. A *critical examination of the requirements for model simulation of wind-induced erosion/deposition phenomena such as snow drifting.* Atmos. Environ. 10: 219-227.
69. Kuipers, H. 1957. *A relief meter for soil cultivation studies.* Netherlands Journal of Agricultural Science 5: 255-262
70. Lascano, R.J., and C.H.M. van Bavel. 1983. *Experimental verification of a model to predict soil moisture and temperature profiles.* Soil Science Society of America Journal 47: 441-448.
71. Lascano, R.J., and C.H.M. van Bavel. 1986. *Simulation and measurement of evaporation from a bare soil.* Soil Science Society of America Journal 50: 1127-1132.
72. Leatherman, S.P. 1978. *A new aeolian sand trap design.* Sedimentology 25: 303-306.
73. Logie, M. 1982. *Influence of roughness elements and soil moisture and resistance of sand to wind erosion.* In: D.H. Yaalon (ed.) *Aridic Soils and Geomorphic Processes.* Catena Supp. 1., 162-173. Braunschweig.
74. Lyles, L. 1976. *Wind patterns and soil erosion in the Great Plains.* In: *Proceedings of the Symposium "Shelterbelts on the Great Plains,"* Great Plains Agriculture Council Publication No. 78. pp. 22-30.
75. Lyles, L. 1983. *Erosive wind energy distributions and climatic factors for the West.* Journal of Soil and Water Conservation 38: 106-109.

76. Lyles, L., and B.E. Allison. 1976. *Wind erosion: The protective role of simulated standing stubble.* Transactions, American Society of Agricultural Engineers 19: 279-283.
77. Lyles, L., J.D. Dickerson, and L.A. Disrud. 1970. *Modified rotary sieve for improved accuracy.* Soil Sci. 109: 207-210.
78. Lyles, L., R.L. Schrandt, and N.F. Schmerdler. 1974. *How aerodynamic roughness elements control sand movement.* Transactions, American Society of Agricultural Engineers 17: 134-139
79. Marshall, T.J., and J.P. Quirk. 1950. *Stability of structural aggregates of dry soil.* Australian Journal of Agricultural Research 1: 266-275.
80. McCauley, J.F., C.S. Breed, P.J. Helm, G.H. Billingsley, and D.J. MacKinnon. 1987. *Monitoring desert winds.* In: John F. McCauley and Jack N. Rinker (eds.) *A workshop on desert processes, September 24-28, 1984 - Report on the conference.* U.S. Geological Survey Circular 989. pp. 6-9.
81. McKinion, J.M., D.N. Baker, J.D. Hesketh, and J.W. Jones. 1975. *Part 4-SIMCOT II: a simulation of cotton growth and yield.* In: *Computer simulation of a cotton production system.* ARS-S-52. p. 27-82.
82. Merva, K.R., and G. Peterson. 1983. *Wind erosion sampling in the North Central Region.* Paper No. 83-2133, Summer Meeting, American Society of Agricultural Engineers, Bozeman, Montana.
83. Nickling, W.G. 1988. *The initiation of particle movement by wind.* Sedimentology 35: 499-511.
84. Peterka, J.A., and J.E. Cermak. 1974. *Simulation of atmospheric flows in short wind tunnel test sections.* Report No. CER73-74JAP-JEC32, Fluid Dynamics and Diffusion Laboratory, Department of Civil Engineering, Colorado St. University, Ft. Collins.
85. Philips, M. 1980. *A force balance model for particle entrainment into a fluid stream.* J. Phys. D: Appl. Phys. 13: 221-233.
86. Potter, K.N. 1990. *Estimation of wind-erodible materials on newly crusted soils.* Soil Sci. (in press).
87. Potter, K.N., T.M. Zobeck, and L.J. Hagen. 1990. *A microrelief index to estimate soil erodibility by wind.* Transactions, American Society of Agricultural Engineers 33(1): 151-155.
88. Radke, J.K., M.A. Otterby, R.A. Young, and C.A. Onstad. 1981. *A microprocessor automated rillmeter.* Transactions, American Society of Agricultural Engineers 24: 401-404, 408.
89. Reed, J.W. 1975. *Wind power climatology of the United States.* SAND 74-0348. Sandia Laboratory, Albuquerque, New Mexico, 163 pp.
90. Rice, C., B.N. Wilson, and M. Appleman. 1988. *Soil topography measurements using image processing techniques.* Computers and Electronics in Agriculture 3: 97-107.
91. Rogowski, A.S., and D. Kirkham. 1976. *Strength of soil aggregates: influence of size, density, and clay and organic matter content.* Med. Fac. Landbouww. Rijksuniv. Gent 41: 85-100.
92. Rogowski, A.S., W.C. Moldenhauer, and D. Kirkham. 1968. *Rupture parameters of soil aggregates.* Soil Science Society of America Proceedings 32: 720-724.

93. Römkens, R.J.M., and J.Y. Wang. 1986. *Effect of tillage on surface roughness.* Transactions, American Society of Agricultural Engineers 29: 429-433.
94. Römkens, R.J.M., J.Y. Wang, and R.W. Darden. 1988. *A laser microrelief meter.* Transactions, American Society of Agricultural Engineers 31: 408-413.
95. Schmidt, R.A. 1977. *A system that measures blowing snow.* U.S. Department of Agriculture Forest Service Research Paper RM-194.
96. Shaw, R.H., and A.R. Pereira. 1982. *Aerodynamic roughness of a plant canopy: A numerical experiment.* Agric. Meteo. 26: 51-65.
97. Skidmore, E.L. 1965. *Assessing wind erosion forces: directions and relative magnitudes.* Soil Science Society of America Proceedings 29: 587-590.
98. Skidmore, E.L. 1986. *Wind erosion climatic erosivity.* Climate Change 9: 195-208.
99. Skidmore, E.L. 1987. *Wind-erosion direction factors as influenced by field shape and wind preponderance.* Soil Science Society of America Journal 51: 198-202.
100. Skidmore, E.L., and L. Dahl. 1978. *Surface soil drying: simulation experiment.* Abstracts for Commission Papers, 11th Congress. International Society of Science, Edmonton, Canada, 1: 246-247.
101. Skidmore, E.L., J.B. Layton, and L.J. Hagen. 1990. *Dry soil-aggregate stability: measuring and relating to wind erosion.* In preparation.
102. Skidmore, E.L., and D.H. Powers. 1982. *Dry soil-aggregate stability: energy-based index.* Soil Science Society of America Journal 46: 1274-1279.
103. Skidmore, E.L., and J. Tatarko. 1991. *Wind in the Great Plains: speed and direction distributions by month.* pp. 195-213. In: J.D. Hanson, M.J. Shaffer, and C.V. Cole (eds.) *Proceedings of the Sustainable Agriculture Symposium.* Fort Collins, Colorado. USDA-ARS-89.
104. Skidmore, E.L., and J. Tatarko. 1990. *Stochastic wind simulation for erosion modeling.* Transactions, American Society of Agricultural Engineers 33(6): 1893-1899.
105. Skidmore, E.L., and N.P. Woodruff. 1968. *Wind erosion forces in the United States and their use in predicting soil loss.* Agricultural Research Service, U.S. Department of Agriculture, Agriculture Handbook No. 346.
106. Soil Conservation Service, U.S. Department of Agriculture. 1988. *National Agronomy Manual.* Second Edition. 190-V Issue I (Part 500-509) SCS, USDA, Washington, D.C.
107. Sorensen, M. 1985. *Estimation of some aeolian saltation transport parameters from transport rate profiles.* Proceedings of the International Workshop on Physics of Blown Sand 1: 141-190. Department of Theoretical Statistics, University of Aarhus, Aarhus, Denmark.
108. Standen, N.M. 1972. *A spire array for generating thick turbulent shear layers for natural wind simulation in wind tunnels.* Report LTR-LA-94, National Aeronautical Establishment, Ottawa, Canada.
109. Steen, B. 1977. *A new simple isokinetic sampler for the determination of particle flux.* Atmos. Environ. 11: 623-627.
110. Stout, J.E., and D.W. Fryrear. 1989. *Performance of a wind blown particle sample.* Transactions, American Society of Agricultural Engineers 32: 2041-2045.

111. Sutherland, R.A., T. Kowalchuk, and E. DeJong. 1991. *Cesium-137 estimates of sediment redistribution by wind.* Soil Sci. 51: 387-396.
112. Toogood, J.A. 1978. *Relation of aggregate stability to property of Alberta soils.* In: W.W. Emerson, R.D. Bond, and A.R. Dexter (eds.) *Modification of Soil Structure.* John Wiley and Sons, New York. pp. 211-215.
113. van Bavel, C.H.M., and D.I. Hillel. 1975. *A simulation study of soil heat and moisture dynamics as affected by a dry mulch.* Proceedings, Summer Computer Simulation Conference 1975. pp. 815-821.
114. van Keulen, H., F.W.T. Penning de Vries, and E.M. Drees. 1982. *A summary model for crop growth.* In: F.W.T. Penning de Vries and H.H. van Laar (eds.) *Simulation of plant growth and crop production.* Simulatio Monogr., Wageningen, Netherlands. p. 87-97.
115. Van Ouwerkerk, C., M. Pot, and K. Boersma. 1982. *Electronic microreliefmeter for seedbed characterization.* Soil Tillage Research 2: 81-90.
116. Wagner, L.E., and Yiming Yu. 1991. Transactions, American Society of Agricultural Engineers 34: 412-416.
117. Wann, M., C.D. Raper Jr., and H.L. Lucas Jr. 1978. *A dynamic model for plant growth: a simulation of dry matter accumulation for tobacco.* Photosynthetica 12: 121-136.
118. Weibull, W. 1951. *A statistical distribution function of wide applicability.* J. Appl. Mech. 18: 293-297.
119. Welch, R., T.R. Jordan, and A.W. Thomas. 1984. *A photogrammatic technique for measuring soil erosion.* Journal of Soil and Water Conservation 39: 191-194.
120. White, B.R. 1982. *Two-phase measurements of saltating turbulent boundary layer flow.* Multiphaser Flow 8: 459-473.
121. White, B.R., and J.C. Schulz. 1977. *Magmes effect on saltation.* J. Fluid Mech. 81: 497-512.
122. Willets, B.B., and M.A. Rice. 1985. *Wind tunnel tracer experiments using dyed sand.* Proceedings, International Workshop on Physics of Blown Sand, 2: 225-242. Department Theoretical Statistics, University of Aarhus, Denmark.
123. Williams, J.R., C.A. Jones, and P.T. Dyke. 1984. *A modeling approach to determining the relationship between erosion and soil productivity.* Transactions, American Society of Agricultural Engineers 27: 129-144.
124. Woodruff, N.P., and F.H. Siddoway. 1965. *A wind erosion equation.* Soil Science Society of America Proceedings 29: 602-608.
125. Zingg, A.W. 1949. *A study of the movement of surface wind.* Agr. Engin. 30: 11-13, 19.
126. Zobeck, T.M. 1989. *Fast-vac, a vacuum system to rapidly sample loose granular material.* Transactions, American Society of Agricultural Engineers 32: 1316-1318.
127. Zobeck, T.M. 1991. *Abrasion of crusted soils: Influence of abrader flux and soil properties.* Soil Science Society of America Journal 55: 1091-1097.